JOURNAL OF NATURAL PRODUCTS

pubs.acs.org/jnp

Article

Bufadienolides from the Eggs of the Toad *Bufo bufo gargarizans* and Their Antimelanoma Activities

Shi-wen Zhou,[#] Jing-yu Quan,[#] Zi-wei Li, Ge Ye, Zhuo Shang, Ze-ping Chen, Lei Wang, Xin-yuan Li, Xiao-qi Zhang, Jie Li,* Jun-shan Liu,* and Hai-yan Tian*

Cite This: https://doi.org/10.1021/acs.jnatprod.0c00840

Read Online

ACCESS | Metrics & More | Article Recommendations | Supporting Information

ABSTRACT: Toads produce potent toxins, named bufadienolides, to defend against their predators. Pharmacological research has revealed that bufadienolides are potential anticancer drugs. In this research, we reported nine bufadienolides from the eggs of the toad *Bufo bufo gargarizans*, including two new compounds (**1** and **3**). The chemical structures of **1** and **3**, as well as of one previously reported semisynthesized compound (**2**), were elucidated on the basis of extensive spectroscopic data interpretation, chemical methods, and X-ray diffraction analysis. Compound **1** is an unusual 19-norbufadienolide with rearranged A/B rings. A biological test revealed that compounds **2** and **4**−**8** showed potent cytotoxic activities toward human melanoma cell line SK-MEL-1 with IC_{50} values less than 1.0 μM. A preliminary mechanism investigation revealed that the most potent compound, **8**, could induce apoptosis via PARP cleavage, while **5** and **6** significantly suppressed angiogenesis in zebrafish. Furthermore, an *in vivo* biological study showed that **5**, **6**, and **8** inhibit SK-MEL-1 cell growth significantly.

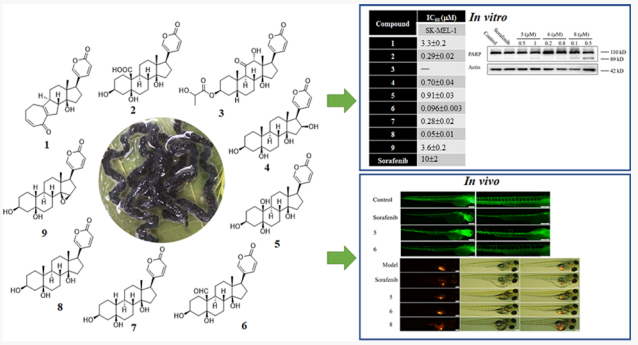

Toads are amphibians and are among the oldest terrestrial vertebrates.[1] As amphibians play a very important role in the evolution of animals and live in a special ecological environment, they have developed their own defense systems.[2] For example, some toads (mainly the genus *Bufo*) produce potent toxins (e.g., bufadienolides) to serve as chemical weapons to fight against their predators.[2] On the other hand, these toad toxins are a valuable resource for medicinal chemistry,[3] as they have been reported to exhibit extensive pharmacological activities such as cytotoxicity,[4,5] local anesthesia,[6] and analgesic[6] and anti-inflammatory effects.[7,8] Bufadienolides are one subclass of cardiac steroids, featuring a basic C_{24} carbon skeleton and a typical 2*H*-pyran-2-one moiety at the C-17 position of the steroidal core. Of the reported activities for the bufadienolides, the cytotoxic effects are the most prominent and have been widely investigated.[4] Bufadienolides from plants and animals have been extensively evaluated for *in vitro* cytotoxic activities against a series of human cancer cell lines, such as leukemia,[9] hepatoma,[10] and lung carcinoma.[11] Mechanism of action studies revealed that they possessed multiple mechanisms on different cancer cells involving induction of apoptosis and cell cycle arrest, inhibition of invasion and metastasis, and reversal of multidrug resistance.[12,13]

In our previous investigations of toad toxins, a series of new bufadienolides were isolated from toad venom and skins, some of which possessed potent hepatocellular carcinoma inhibitory effects.[10] Motivated by previous reports that the early morphology of toads, the eggs, harbor more diverse and toxic bufadienolides than the adults, as they cannot move freely and might need more powerful chemical defenses to fight against natural enemies, we have carried out a systematic chemical investigation on toad eggs in recent years, leading to the isolation of a series of unique bufadienolides conjugated with either a terminal hydroxy fatty acid or D/L-lactic acid.[11,14,15] As part of our continuing search for structurally intriguing and biologically active compounds from toad eggs, nine bufadienolides (**1**−**9**) including two new compounds (**1** and **3**) were obtained. Because compound **2** was only synthesized in a Chinese patent and no relevant spectroscopic data were published,[16] we report the isolation and structure elucidation of **2** along with the new compounds **1** and **3**. *In vitro* and *in vivo* antimelanoma effects, antiangiogenic activities, and cardiac toxicities of these bufadienolides were also evaluated.

Received: July 28, 2020

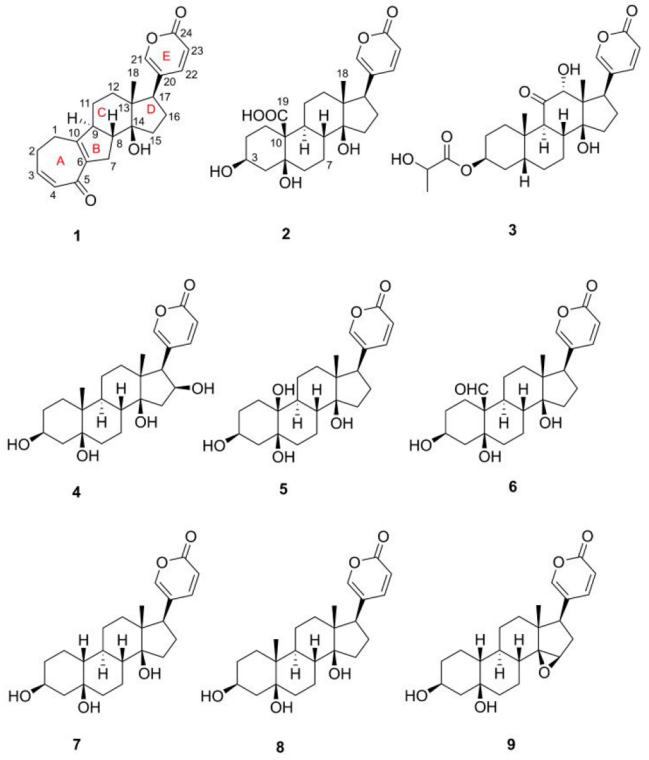

RESULTS AND DISCUSSION

The 95% EtOH extract of the eggs of the toad *Bufo bufo gargarizans* was partitioned with cyclohexane and EtOAc. Compounds **1**−**9** were obtained from the EtOAc partition by a series of column chromatographic separations and the preparative HPLC method (detailed isolation procedure, Experimental Section).

Compound **1** was obtained as a white amorphous powder. The molecular formula of **1** was established to be $C_{23}H_{27}O_4$ by its HRESIMS data, indicating the presence of 11 degrees of unsaturation. The UV absorption maxima at 240 and 300 nm revealed the existence of a 2*H*-pyran-2-one moiety and an additional conjugated system. The IR spectrum suggested the presence of hydroxy (3382 cm^{-1}) and carbonyl (1718 cm^{-1}) groups. The ^1H NMR spectrum showed three characteristic signals for a 2*H*-pyran-2-one moiety [δ_H 6.30 (1H, d, J = 9.7 Hz), 7.45 (1H, d, J = 2.6 Hz), and 8.25 (1H, dd, J = 9.7, 2.6 Hz)], two olefinic protons [δ_H 6.70 (1H, m) and 6.05 (1H, d, J = 13.3 Hz)], and one angular methyl [δ_H 0.75 (3H, s)]. The analysis of ^{13}C NMR and DEPT spectra revealed 23 carbon signals, including seven nonprotonated carbons, eight methine carbons, seven methylene carbons, and one methyl carbon, among which one carbon signal at δ_C 192.3 and five characteristic carbon signals at δ_C 115.6, 124.8, 149.2, 150.4, and 164.7 were attributable to a keto carbonyl and a 2*H*-pyran-2-one ring, respectively. This above information suggested **1** was a bufadienolide derivative. Comparison of the ^1H and ^{13}C NMR data of **1** with those of the known compound bufalin indicated **1** had the same substructure as bufalin in rings C, D, and E (Table 1, Figures S34−S39, Supporting Information).[17]

Further structural information on **1** came from the inspection of the COSY spectrum, which demonstrated four isolated spin systems (Figure 1a). The HMBC correlations between H_2-2/H-7β/H-9 and C-10, H-3/H-7β and C-5, and H_2-1/H-4/H-8 and C-6 revealed rings A and B were connected via a C-6 to C-10 bond, thus generating a 5/7

Table 1. ^1H and ^{13}C NMR Data of Compound 1 and Bufalin (CD_3OD, δ in ppm)

	1		bufalin	
position	δ_C,[a] type	δ_H[b] (J in Hz)	δ_C,[a] type	δ_H[b] (J in Hz)
1α	27.2, CH_2	2.49[c]	30.8, CH_2	1.47[c]
1β		2.49[c]		1.47[c]
2α	27.1, CH_2	2.42, m	28.6, CH_2	1.62[c]
2β		2.49[c]		1.49[c]
3	144.8, CH	6.70, m	67.7, CH	4.06, br s
4α	134.1, CH	6.05, dd (12.1, 1.3)	34.2	1.33[c]
4β				1.96, m
5	192.3, C		37.4	1.78[c]
6α	140.5, C		27.9	1.26, m
6β				1.91, m
7α	33.2, CH_2	2.19[c]	22.6	1.43[c]
7β		2.73, dd (14.7, 6.7)		1.82, m
8	51.9, CH	1.89, m	43.0, CH	1.64[c]
9	53.8, CH	2.57, m	36.9, CH	1.72[c]
10	164.2, C		36.5, C	
11α	26.5, CH_2	1.86, m	22.6, CH_2	1.19[c]
11β		1.36, m		1.30[c]
12α	43.6, CH_2	1.57, m	42.0, CH_2	1.47[c]
12β		1.69, dt (13.8, 3.2)		1.47[c]
13	54.9, C		49.6, C	
14	84.5, C		86.2, C	
15α	33.0, CH_2	2.19[c]	33.2, CH_2	2.09, m
15β		1.75, dd (12.4, 8.2)		1.71
16α	30.9, CH_2	2.23, m	29.9, CH_2	2.19, m
16β		1.83, m		1.72[c]
17	51.9, CH	2.63, dd (7.2, 9.0)	52.3, CH	2.55,dd (9.5, 6.2)
18	17.8, CH_3	0.75, s	17.3, CH_3	0.71, s
19			24.3, CH_3	0.96, s
20	124.8, C		122.7, C	
21	150.4, CH	7.45, d (2.6)	149.2, CH	7.42, d (2.5)
22	149.2, CH	8.00, dd (2.6, 9.7)	147.4, CH	7.99, dd (2.5, 9.7)
23	115.6, CH	6.30, d (9.7)	114.3, CH	6.27, d (9.7)
24	164.7, C		161.4, C	

[a]Measured at 125 MHz. [b]Measured at 500 MHz. [c]Overlapped signals were reported without designating multiplicity.

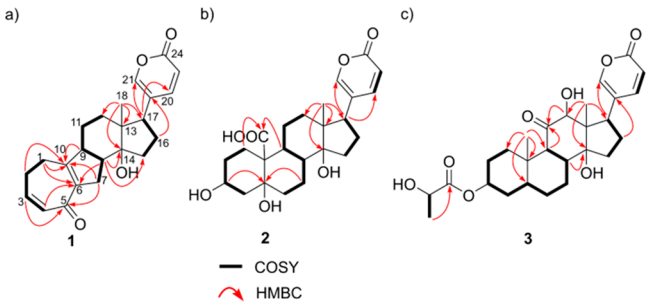

Figure 1. Key HMBC and COSY correlations of **1**−**3**.

ring system. Moreover, the HMBC correlations between H-8 and C-15 and between H_2-11 and C-10 indicated rings B and C were connected through C-8 and C-9. Thus, the planar structure of **1** was established to be a rare 19-norbufadienolide with a 7/5/6/5/6 carbon skeleton as shown in Figure 1a. The relative configuration of **1** was determined by interpretation of ROESY data. The strong NOE correlations between H-8/H-11β and H_3-18 indicated that H-8, H-11β, and CH_3-18 occupied the axial positions of ring C in a chair conformation

https://doi.org/10.1021/acs.jnatprod.0c00840
J. Nat. Prod. XXXX, XXX, XXX−XXX

and were designated as β-orientation. Accordingly, the NOE correlations between H-9/H-17 and H-12α indicated those protons were cofacial and α-oriented. In addition, the strong NOE correlations between H-9/H-12α and H-15α supported the common *cis*-fused configurations of C and D rings (Figure 2).[3] Noting the typical 17β position of the lactone ring, as well

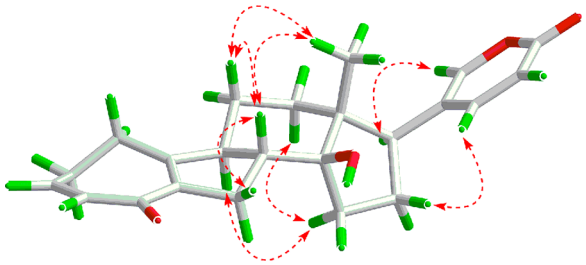

Figure 2. Key NOE correlations of **1**.

as the corresponding 17*R* configuration of bufadienolides, the absolute configurations of **1** are proposed to be 8*R*, 9*S*, 13*R*, 14*S*, and 17*R*. Therefore, the completed structure of **1** was established and given the trivial name bufogargarizin D. Compound **1** features an unusual C_{23} skeleton with a 7/5/6/5/6 ring system, which is distinctly different from the common C_{24} skeleton for 6/6/6/5/6 ring system bufadienolides. So far, only six A/B ring rearranged bufadienolides have been reported, and five of them were discovered by our research group.[18−21] A biosynthesis pathway was proposed in our previous research, involving the oxidation of the vicinal diols in the precursor compound **5**, followed by an intramolecular aldol condensation to form the 7/5 or 5/7 A/B ring system.[18] The highly unsaturated 7/5 rings in **1** can be formed by further dehydration (Scheme S1, Supporting Information).

Compound **2**, colorless blocks, had the molecular formula $C_{24}H_{32}O_7$ as established by its HRESIMS data, indicating 10 degrees of unsaturation. The UV and IR data were consistent with a bufadienolide derivative. Comparison of ^{1}H and ^{13}C NMR signals of **2** (Table 2) with those of the known compound hellebrigenin (**6**) revealed their structures are very similar except for the presence of a carboxyl (δ_C 178.0) rather than a formyl group at C-19 (Table S8, Figures S52−S54, Supporting Information),[22] which was subsequently confirmed by the HMBC correlations between H-1β/H-9 and C-19 and its molecular formula. On the basis of the extensive analysis of COSY, HSQC, HMBC, and ROESY spectra, the ^{1}H and ^{13}C NMR signals of **2** were assigned (Figure 1b and Table 2). In addition, an X-ray diffraction experiment established the absolute configuration of **2** (Figure 3) with the final refined Flack parameter of 0.10(5) and Hooft parameter of 0.12(4). Consequently, **2** was determined to be (3β,5β,14β)-3,5-dihydroxy-10-carboxybufa-20,22-dienolide and given a trivial name of 19-carboxy-19-demethyltelocinobufagin.

Compound **3** was isolated as an amorphous solid. Its molecular formula was deduced to be $C_{27}H_{36}O_8$ based on a sodium adduct ion peak at *m*/*z* 511.2305 in its HRESIMS spectrum. The ^{1}H NMR spectrum showed characteristic signals for a 2*H*-pyran-2-one ring, and the ^{13}C NMR and DEPT spectra indicated **3** possesses 27 carbon signals. The typical NMR signal for a secondary methyl [δ_H 1.39 (3H, d, *J* = 6.9 Hz) and δ_C 20.7], a methine [δ_H 4.25 (1H, q, *J* = 6.9 Hz) and δ_C 68.0], and an ester carbonyl (δ_C 175.9) were attributable to a lactate unit,[11] which was further confirmed

Table 2. ^{1}H and ^{13}C NMR Data of Compounds 2 and 3 (CD_3OD, δ in ppm)

	2		3	
position	δ_C,[a] type	δ_H[b]	δ_C,[a] type	δ_H[b]
1α	21.4, CH_2	1.82, br d (14.9)	32.0, CH_2	1.44, m
1β		2.38, m		1.88, m
2α	28.4, CH_2	1.68[c]	31.8, CH_2	1.32, m
2β		1.68[c]		1.51, m
3	68.1, CH	4.12, br s	72.6, C	5.15, br s
4α	39.1, CH_2	2.18[c]	34.6, CH_2	1.69[c]
4β		1.55[c]		1.69[c]
5	75.6, C		38.7, CH	1.73, m
6α	37.0, CH_2	1.43[c]	26.3, CH_2	1.66[c]
6β		2.42[c]		1.98, m
7α	24.5, CH_2	1.29, m	21.9, CH_2	1.34[c]
7β		2.01, m		1.92[c]
8	41.7, CH	2.22, m	40.9, CH	2.42, m
9	40.1, CH	1.64[c]	47.0, CH	2.54, d (12.3)
10	55.6, C		38.8, CH	1.74, m
11α	24.6, CH_2	1.63[c]	215.6, C	
11β		1.36[c]		
12α	41.9, CH_2	1.53[c]	84.0, CH	4.16, s
12β		1.45[c]		
13	49.7, C		55.7, C	
14	86.0, C		84.3, C	
15α	32.7, CH_2	2.05[c]	28.1, CH_2	1.99[c]
15β		1.68[c]		1.94[c]
16α	29.8, CH_2	2.19[c]	28.6, CH_2	1.69[c]
16β		1.75, m		1.32[c]
17	52.0, CH	2.54, dd (9.6, 6.5)	47.6, CH	2.49, m
18	17.3, CH_3	0.72, s	19.3, CH_3	0.98, s
19	178.0, C		24.7, CH_3	1.05, s
20	125.0, C		121.7, C	
21	150.5, CH	7.43, d (2.5)	152.5, CH	7.52, d (2.6)
22	149.3, CH	7.99, dd (9.7, 2.5)	149.8, CH	7.70, dd (9.7, 2.6)
23	115.4, CH	6.27, d (9.7)	114.5, CH	6.24, d (9.7)
24	164.8, C		164.6, C	
1′			175.9, C	
2′			68.0, CH	4.25, q (6.9)
3′			20.7, CH_3	1.39, d (6.9)

[a]Measured at 125 MHz. [b]Measured at 500 MHz. [c]Overlapped signals were reported without designating multiplicity.

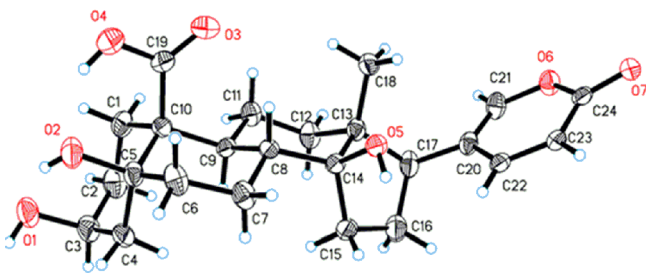

Figure 3. X-ray ORTEP drawing of **2**.

by the COSY correlation of H-2′ and H_3-3′ and HMBC correlation between H_3-3′ and C-1′. Comparison of ^{1}H and ^{13}C NMR data for the protons and carbons in the steroidal nucleus with the known compound ψ-bufarenogin[23] indicated they were nearly the same, except for the deshielded shift for H-3 (δ_H 5.15, br s) and C-3 (δ_C 72.6). This above information suggested **3** was the lactate conjugate of ψ-bufarenogin.

https://doi.org/10.1021/acs.jnatprod.0c00840
J. Nat. Prod. XXXX, XXX, XXX−XXX

We previously showed that bufadienolide lactate conjugates exist as stereoisomers due to the epimerization of the C-2′ stereogenic center.[11] However, the ^{1}H NMR spectrum of **3** did not exhibit split signals for the doublet methyl group in the lactate moiety, and the chiral-phase HPLC chromatogram did not show two eluting peaks as for our previously isolated bufadienolide lactate conjugates.[11] Then we selected (*S*)-MTPA-Cl to react with **3**, and it was surprising that the doublet methyl protons showed obvious splitting signals in the ^{1}H NMR spectrum of the product, indicating the existence of two epimers (Figure S32, Supporting Information). The deshielded shift for H-2′ (δ_H 5.65) verified the successful esterification of the hydroxy group at C-2′. Then we conducted another chiral-phase HPLC analysis, which displayed two closely eluting peaks (Figure S33, Supporting Information). A preparative chiral-phase HPLC separation yielded two MTPA esters of **3** (**3a** and **3b**). After a comparison of their ^{1}H NMR spectra, **3a**, with a relatively shielded chemical shift of H_3-3′ and deshielded chemical shift of H-3, was determined to be the (*R*)-MTPA ester of the D-lactate conjugate of ψ-bufarenogin. By contrast, **3b**, with a relatively deshielded chemical shift of H_3-3′ and shielded chemical shift of H-3, was deduced to be the (*R*)-MTPA ester of the L-lactate conjugate of ψ-bufarenogin.

The known compounds (3β,5β,14β,16β)-3,5,14,16-tetrahydroxybufa-20,22-dienolide (**4**),[24] (3β,5β,14β)-3,5,10,14-tetrahydroxy-19-norbufa-20,22-dienolide (**5**),[21] hellebrigenin (**6**),[25] (3β,5β,14β)-3,5,14-trihydroxy-19-norbufa-20,22-dienolide (**7**),[19] telocinobufagin (**8**),[25] and (3β,5β,10β)-3,5-dihydroxy-14,15-epoxy-19-norbufa-20,22-dienolide (**9**)[15] were identified by comparison with literature spectroscopic data (Figures S43−S69).

Bufadienolides have been reported to be potent cytotoxic agents against an array of malignant cancer cells.[4] However, their effects on human melanoma cells have been rarely reported.[26,27] Melanoma is the most aggressive form of skin cancer and frequently resists chemotherapy.[28] In this study, all of the isolated compounds except **3**, due to a limited amount, were evaluated for cytotoxic activities against the human melanoma cell line SK-MEL-1 (Table 3). The results showed that compounds **2** and **4**−**8** showed potent cytotoxic activities against the SK-MEL-1 cells with IC_{50} values less than 1.0 μM. Compounds **1** and **9** were less toxic, with IC_{50} values of 3.3 ± 0.2 and 3.6 ± 0.2 μM, respectively. A structure−activity relationship (SAR) analysis revealed that the bufadienolides of the 14β-hydroxy type (**2**, **4**−**8**) are much more potent than those of the 14,15-epoxy type (**9**), which was consistent with previous SAR studies of bufadienolides.[29] It should be pointed out that although **1** contains a 14β-hydroxy group, the activity is still weak, which may be caused by the rearrangement of the basic steroidal rings A and B.

Table 3. Cytotoxic Activities of Isolated Compounds in Human Melanoma SK-MEL-1 Cells[a]

	IC_{50} (μM)
compound	SK-MEL-1
1	3.3 ± 0.2
2	0.29 ± 0.02
3	
4	0.70 ± 0.04
5	0.91 ± 0.03
6	0.096 ± 0.003
7	0.28 ± 0.02
8	0.05 ± 0.01
9	3.6 ± 0.2
sorafenib[b]	10 ± 2

[a]All results are presented as means ± SD at three independent experiments. [b]Sorafenib was used as the positive control.

PARP is one of the most important apoptosis biomarkers, as it can be cleaved in the event of apoptosis.[30] In order to evaluate whether bufadienolides induced apoptosis, we examined the protein expression level of PARP in SK-MEL-1 cells after bufadienolide treatment. Results showed that **8** decreased the level of PARP while the cleaved PARP was accumulated, suggesting that **8** induced cell apoptosis. However, this phenomenon was not observed after **5**, **6**, or sorafenib treatment, inferring that these compounds may exert antitumor activities through cell cycle arrest or other mechanisms (Figure 4).

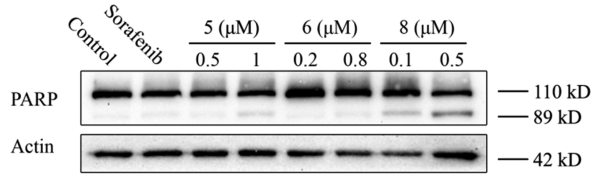

Figure 4. Compounds **5**, **6**, and **8** induce the cleavage of PARP. SK-MEL-1 cells were treated with **5**, **6**, and **8** for 48 h. The protein expression level of PARP was examined by Western blotting. β-Actin was used as a loading control. Sorafenib (10 μM) was used as the positive control.

On the basis of these results, we further explored alternative antitumor mechanisms of the isolated bufadienolides. The blockage of angiogenesis is considered as a highly effective approach in cancer treatment, because the process of angiogenesis supports necessary nutrients and oxygen to stimulate cancer growth, invasion, and metastasis.[31] The zebrafish model, a novel and attractive tool for drug screening due to low cost, easy observation, and high homology with human genotype, is a suitable choice for angiogenesis screening.[32−34] Therefore, we used transgenic *Tg*(*fli1:GFP*) and *Tg*(*flk1:GFP*) zebrafish embryos to evaluate the effects of the isolates on vascular generation. In the process of angiogenesis, the vessels form via the sprouting. Inhibition of angiogenesis resulted in a decrease in the numbers of angiogenic sprouts and complete intersegmental blood vessels (ISVs) in zebrafish. By evaluating the number of angiogenic sprouts and complete ISVs in zebrafish trunk and tail during development, we can directly judge the effect of drugs on angiogenesis.[35] According to stereo fluorescence microscopy, the ISVs and the sprouts of embryos in the control group were abundant and clear. Compared with the control group, the treatment with compounds **5** and **6** obviously decreased the numbers of ISVs and the sprouts in *Tg*(*fli1:GFP*) zebrafish embryos with the activity of **5** stronger than that of **6**, which indicates that these two compounds exert potent antiangiogenic effects. However, the ISVs and the sprouts in zebrafish embryos treated with compounds **1**, **2**, **4**, **8**, and **9** showed no obvious difference compared with the control group, suggesting that these compounds have no antiangiogenic effect on the transgenic zebrafish embryos (Figure 5). The main structural differences of **2**, **5**, **6**, and **8** were their

https://doi.org/10.1021/acs.jnatprod.0c00840
J. Nat. Prod. XXXX, XXX, XXX−XXX

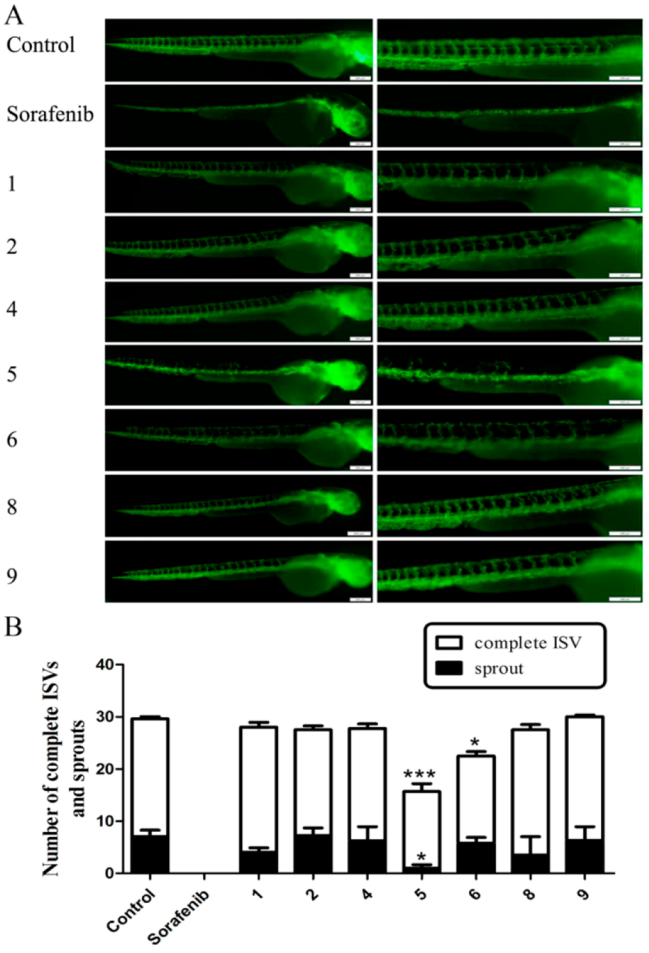

Figure 5. Compounds **5** and **6** exhibit significant antiangiogenic effects *in vivo*. Zebrafish embryos (*Tg:Fli1-GFP*) at 12 h postfertilization (hpf) were selected and treated with isolates (20 μM). At 24 hpf, the embryo membranous eggshells were broken. At 48 hpf, the development of embryonic blood vessels was observed under a fluorescence microscope (A), and the numbers of intersegmental vessels (ISVs) and sprout angiogenesis were counted (B). *$P < 0.05$, ***$P < 0.01$ versus control, one-way ANOVA, *post hoc* comparisons, Tukey, columns, mean; error bar, SD. Sorafenib (1 μM) was used as the positive control.

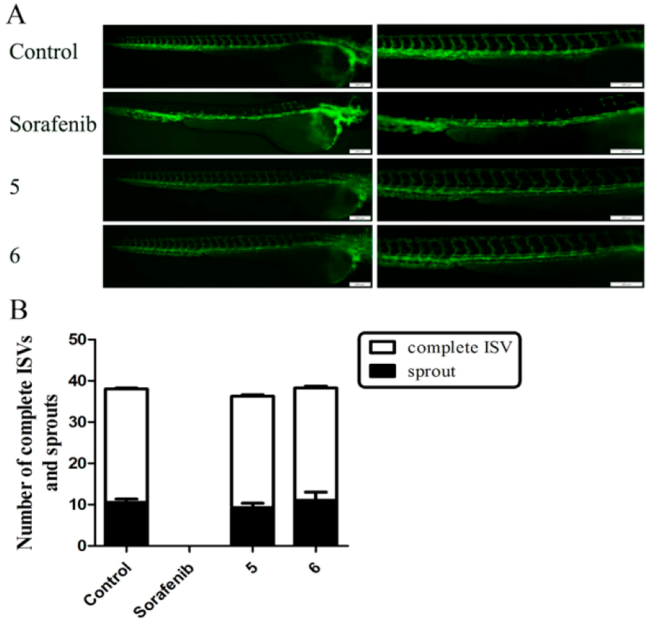

Figure 6. Compounds **5** and **6** have no obvious effect on transgenic zebrafish (*Tg:Flk1-GFP*). Zebrafish embryos at 12 h postfertilization (hpf) were selected and treated with **5** (20 μM) and **6** (20 μM). At 24 hpf, the embryo membranes were broken. At 48 hpf, the development of embryonic blood vessels was observed under a fluorescence microscope (A) and the numbers of intersegmental vessels (ISVs) and sprout angiogenesis were counted (B). One-way ANOVA, *post hoc* comparisons, Tukey, columns, mean; error bar, SD. Sorafenib (1 μM) was used as the positive control.

substituents at the C-10 position, indicating this should be a key factor influencing their activities. A SAR analysis revealed that a hydroxy or an aldehyde group at C-10 is favorable for their antiangiogenic effect, while a carboxy or methyl group at C-10 will decrease their activities.

It is well accepted that vascular endothelial growth factors (VEGFs) and their ligands are necessary in angiogenesis. Research found that the disruption of endothelial-specific *flk1* (encoding VEGFR2) could attenuate the generation or function of vessels at the sprouting stage of angiogenesis.[36] Therefore, we further explored whether compounds **5** and **6** attenuated angiogenesis through the inhibition of VEGFR2. However, the results showed that **5** and **6** had no obvious influence on the generation of ISVs compared with the control group in *Tg*(*flk1:GFP*) zebrafish, suggesting that the antiangiogenic effect of these two compounds is due to another mechanism (Figure 6).

The xenotransplantation of cancer cells in zebrafish is a suitable platform for anticancer drug discovery because it can closely simulate human clinical cancer without causing immunosuppression.[37] As described previously, human melanoma cells microinjected into the yolk sac of zebrafish embryos could proliferate and form masses *in vivo*.[38] Considering that **5** and **6** inhibit angiogenesis and **8** showed the most potent *in vitro* antitumor activity, we speculated that they might also exert *in vivo* antitumor effects. Zebrafish xenograft results demonstrate that all these compounds inhibit SK-MEL-1 cells *in vivo*, and compound **8** exerts the most significant activity. However, the antitumor effects of compounds **5**, **6**, and **8** are weaker than that of Sorafenib (Figure 7).

As bufadienolides are known to be cardiotoxic, we tested cardiac toxicities of our isolated compounds in zebrafish.[3] Compounds **1**, **8**, and **9** exerted obvious toxicities, including death, pericardial edema, curved tail, etc. Compounds **5** and **6** were less toxic to zebrafish, but **6** induced pericardial edema in zebrafish larvae at the concentration of 100 μM, which indicates that **6** has cardiotoxicity in zebrafish larvae. However, **2** and **4** showed no toxicity in zebrafish at the concentration of 100 μM (Figure 8). In comparison with *in vivo* antitumor results, we found that bufadienolides exhibited significant antitumor activities at a relatively safe dose.

In summary, two new bufadienolides (**1** and **3**), along with seven known analogues (**2** and **4**–**9**), were isolated from the eggs of the toad *B. bufo gargarizans*. In our previous study, we discovered two novel A/B ring rearranged bufadienolides in toad venom.[18] It is interesting that in the early morphology of toads the eggs can also contain such interesting molecules like compound **1**. Furthermore, we have found that 19-nor bufadienolides also exist in toad eggs (**5**, **7**, and **9**), which have previously been isolated from toad venom as trace ingredients by our group.[39] Bioactivity results showed that

https://doi.org/10.1021/acs.jnatprod.0c00840
J. Nat. Prod. XXXX, XXX, XXX−XXX

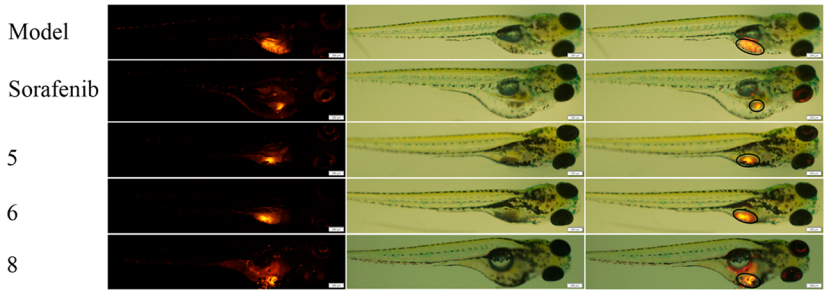

Figure 7. Compounds **5**, **6**, and **8** exert antimelanoma effects *in vivo* by CM-Dil staining. Melanoma cells SK-MEL-1 prestained by CM-Dil dye (2 μM) were microinjected into the yolk of zebrafish and treated with **5** (20 μM), **6** (20 μM), and **8** (10 μM) for 48 h. CM-Dil fluorescence was observed by microscopy. Sorafenib (0.5 μM) was used as the positive control. Left: CM-Dil-staining cells, middle: bright field, right: merge. The black oval area indicates the melanoma area.

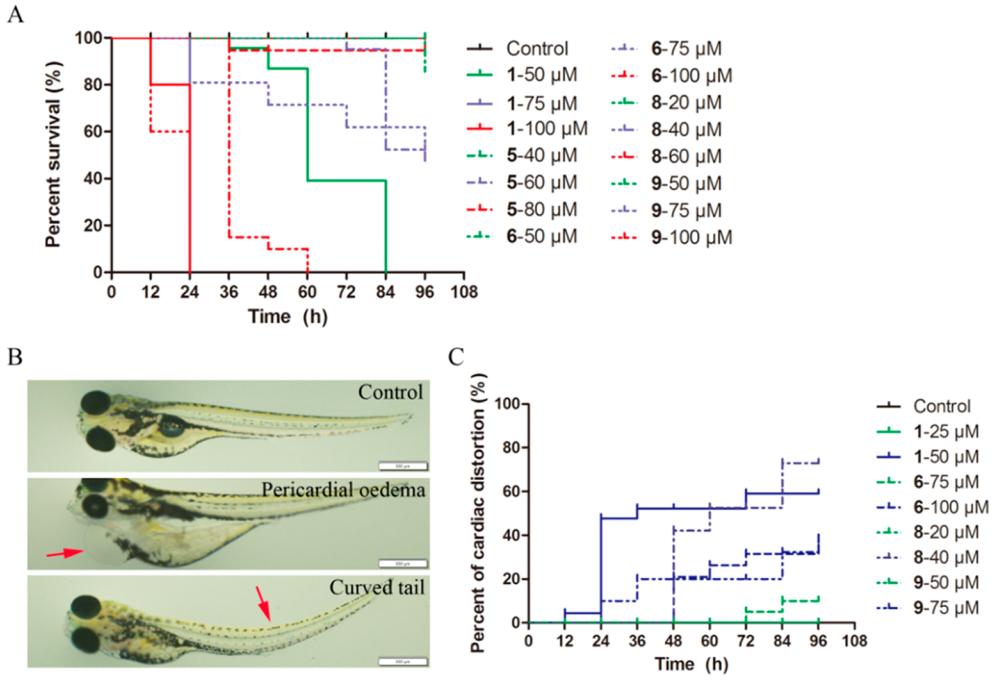

Figure 8. Toxicity of **1**, **5**, **6**, **8**, and **9** in zebrafish larvae. Zebrafish larvae at 48 hpf were treated with compounds **1**, **5**, **6**, **8**, and **9** and then were observed by a stereomicroscope (Olympus SZX7) every 12 h. (A) Survival analysis on zebrafish larvae treated with compounds **1**, **5**, **6**, **8**, and **9**. (B) Pathological changes in zebrafish larvae, including pericardial edema and curved tail, were observed under the light field of a stereomicroscope. The red arrow points to the pericardial edema and curved tail. (C) Percent of cardiac distortion in zebrafish larvae.

compounds **2** and **4**–**8** showed potent cytotoxic activities against SK-MEL-1 cells with IC_{50} values in the submicromolar range. Moreover, preliminary mechanism of action studies showed that compound **8**, with the most potent activity, could cause PARP cleavage, indicating that it might kill cancer cells via apoptosis. To our surprise, of all the tested bufadienolides, only **5** and **6** significantly suppressed angiogenesis. And a further *in vivo* study revealed that **5**, **6**, and **8** inhibited the growth of SK-MEL-1 cells in zebrafish, indicating that bufadienolides with different structures exert their antitumor effects via different mechanisms. Finally, it is worth mentioning that a substantial difference in structure can lead to significant changes in toxicities of bufadienolides. Comparing their cytotoxic effects with cardiac toxicities, we found that bufadienolides have a variable safety index. However, the structure–activity relationship of their antitumor effects and cardiotoxicities and their mechanisms of cytotoxicity require further exploration.

EXPERIMENTAL SECTION

General Experimental Procedures. The optical rotations were measured on a JASCO digital polarimeter using a thermostable optical glass cell (0.1 dm path length and *c* in g/100 mL). UV spectra were determined on a JASCO V-550 UV/vis spectrometer. IR spectra were acquired on a JASCO FT-IR-4600 infrared spectrometer in KBr pellets. All NMR spectra were recorded on a Bruker AV-400/500 spectrometer using the residual signals (CD_3OD: δ_H 3.31/δ_C 49.0) as the internal standard. HRESIMS were obtained on an Agilent 6210 HPLC TOF mass spectrometer. HPLC was performed on an Agilent 1200 HPLC system equipped with a diode array detector, using a biphenyl column (Kinetex Biphenyl, 5 μm, 4.6 × 250 mm, Phenomenex) and a preparative chiral-phase column (Lux Cellulose-4, 5 μm, 4.6 × 250 mm, Phenomenex) for analysis. Pre-HPLC was conducted on a Wufeng L-100 HPLC system (Wufeng Corporation), using a biphenyl preparative column (Kinetex Biphenyl, 10 μm, 10 × 250 mm, Phenomenex) and a chiral-phase preparative column (Lux Cellulose-4, 10 μm, 10 × 250 mm, Phenomenex) for preparative purification. Open column chromatography (CC) was operated on reversed-phase C_{18} silica gel (YMC Corporation) and silica gel (200–300 mesh, Haiyang Chemical

https://doi.org/10.1021/acs.jnatprod.0c00840
J. Nat. Prod. XXXX, XXX, XXX−XXX

Group Corporation). X-ray single-crystal diffraction data for compounds were collected on a Rigaku X-ray diffractometer at 100(10) K. Sorafenib was purchased from Aladdin (Shanghai, China). PARP antibody was purchased from Santa Cruz Biotechnology. Cell tracker CM-Dil was purchased from Yeasen. Other reagents were obtained from Sigma-Aldrich.

Animal Material. The eggs of *B. bufo gargarizans* were purchased from Dongtai Toad Breeding Base in Jiangsu Province of China between March and May, 2015, and authenticated by Professor Guang-Xiong Zhou (Institute of Traditional Chinese Medicine & Natural Products, Jinan University, Guangzhou, People's Republic of China). A voucher specimen (No. 201503031) was deposited in the Institute of Traditional Chinese Medicine and Natural Products, College of Pharmacy, Jinan University.

Extraction and Isolation. The air-dried and roughly powdered eggs of *B. bufo gargarizans* (25 kg) were extracted with 95% EtOH at room temperature under ultrasonication three times. After removal of the solvent under reduced pressure at 40 °C, the extract (2.5 kg) was suspended in 20% aqueous MeOH (20 L) and subsequently partitioned against cyclohexane (3 × 20 L) and EtOAc (3 × 20 L). The concentrated EtOAc layer (253 g) was subjected to silica gel (200−300 mesh), eluted with CH_2Cl_2/MeOH gradients (100:1, 50:1, 20:1, and 10:1) to give 16 fractions (Fr. 1−16). Fr. 5 (11.2 g) was chromatographed over a reversed-phase C18 silica column eluted with MeOH/H_2O gradients (1:1 → 10:1) to yield five fractions (Fr. 5.1−5.5). Fr. 5.1 (1.2 g) and Fr. 5.2 (1.5 g) were further purified on an RP-biphenyl HPLC (MeOH/H_2O: 85%, flow rate: 5 mL/min) to afford **1** (1.7 mg, t_R: 45 min) and **3** (1.6 mg, t_R: 51 min), respectively. Fraction 5.3 (226 mg) was subjected to silica gel CC eluted with CH_2Cl_2/MeOH gradients (1:10 → 1:1) to give **9** (4.3 mg). Fr. 6 (9.5 g) was applied to silica gel CC eluted with CH_2Cl_2/MeOH gradients (1:8 → 1:1) to give **6** (5.3 mg), **7** (5.9 mg), and **8** (5.6 mg). Fr. 8 (8.1 g) was chromatographed over a reversed-phase C18 silica column eluted with MeOH/H_2O gradients (2:3 → 10:1) and further purified by RP-biphenyl HPLC (MeOH/H_2O: 65%, flow rate: 5 mL/min), affording **5** (10.5 mg, t_R: 27 min) and **2** (8.8 mg, t_R: 35 min). Similarly, Fr. 9 (9.6 g) was subjected to a reversed-phase C18 silica column eluted with MeOH/H_2O gradients (3:7 → 10:1) and then RP-biphenyl HPLC (MeOH/H_2O: 60%, flow rate: 5 mL/min) giving **4** (5.0 mg, t_R: 33 min).

*Bufogargarizin D (**1**):* white amorphous powder; $[\alpha]^{25}_D$ +28 (*c* 0.10, MeOH); UV (MeOH) λ_{max} (log ε) 204 (3.62), 236 (3.47), and 300 (3.52) nm; IR (KBr) ν_{max} 3384, 2928, 1716, 1596, 1089 cm^{-1}; ^1H (500 MHz, CD_3OD) and ^{13}C NMR (125 MHz, CD_3OD) data, Table 1; HRESIMS *m*/*z* 367.1908 $[M + H]^+$ (calcd for $C_{23}H_{27}O_4$, 367.1904).

*19-Carboxy-19-demethyltelocinobufagin (**2**):* colorless plates (MeOH); mp 186−187 °C; $[\alpha]^{25}_D$ +18 (*c* 0.10, MeOH); UV (MeOH) λ_{max} (log ε) 205 (3.96), 300 (3.71) nm; IR (KBr) ν_{max} 3409, 2932, 1708, 1537, 1448, 1245, 1136 cm^{-1}; ^1H (500 MHz, CD_3OD) and ^{13}C NMR (125 MHz, CD_3OD) data, Table 2; HRESIMS *m*/*z* 433.2220 $[M + H]^+$ (calcd for $C_{24}H_{33}O_7$, 433.2221).

*ψ-Bufarenogin-3-O-lactate (**3**):* white amorphous powder; $[\alpha]^{25}_D$ +60 (*c* 0.10, MeOH); UV (MeOH) λ_{max} (log ε) 205 (4.18), 299 (4.08) nm; IR (KBr) ν_{max} 3425, 3384, 2946, 1705, 1694, 1536, 1031 cm^{-1}; ^1H (500 MHz, CD_3OD) and ^{13}C NMR (125 MHz, CD_3OD) data, Table 2; HRESIMS *m*/*z* 511.2305 $[M + Na]^+$ (calcd for $C_{27}H_{36}O_8Na$, 511.2302).

X-ray Crystallographic Analysis. Compound **2** was obtained as colorless blocks from MeOH. A suitable single crystal of **2** was selected for single-crystal X-ray diffraction analysis. The intensity data were collected at a temperature of 100 K on a SuperNova, Dual, Cu at zero, AtlasS2 diffractometer by using mirror monochromatic Cu Kα radiation (λ = 1.54184 nm). Data processing was accomplished with Olex2 and SHELXTL crystallographic software packages.[40] The structure was solved with the ShelXS structure solution program using direct methods and refined with the ShelXL refinement package using least squares minimization.[41,42] Crystallographic data (excluding structure factor tables) for **2** (CCDC 2012338) have been deposited in the Cambridge Crystallographic Data Centre.

*Crystallographic data for compound **2**:* $C_{48}H_{66}O_{15}$, M = 883.00 g/mol, monoclinic, space group $P2_1$, a = 13.7133(2) Å, b = 12.14470(10) Å, c = 13.78260(10) Å, β = 109.4670(10)°, V = 2164.19(4) $Å^3$, Z = 2, T = 100.00(10) K, μ(Cu Kα) = 0.824 mm^{-1}, D_x = 1.355 g/cm^3, 41 331 reflections measured (6.802° ≤ 2θ ≤ 147.376°), 8609 unique (R_{int} = 0.0390, R_{sigma} = 0.0257), which were used in all calculations. The final R_1 was 0.0354 [$I > 2\sigma(I)$] and wR_2 was 0.1151 (all data). The goodness of fit on F^2 was 0.998. Flack parameter = 0.10(5).

Mosher's Ester Formation of 3a/3b. The modified Mosher's method was carried out as previously described.[11] Briefly, **3** (0.88 mg) was dried under vacuum conditions for 24 h and dissolved in deuterated pyridine (pyridine-d_5) (500 μL). (*S*)-MTPA-Cl (15 μL) was subsequently added under an atmosphere of nitrogen at room temperature. The solutions were mixed completely and reacted at room temperature for 24 h. Then the mixture was separated by a preparative Cellulose-4 chiral-phase HPLC (MeOH/H_2O: 70% → 90%, 30 min, flow rate: 5 mL/min) to yield two MTPA esters of **3** (**3a** and **3b**). Each of them was subsequently analyzed by NMR spectroscopy.

Cell Culture. Human melanoma cells SK-MEL-1 were purchased from American Type Culture Collection. The cells were cultured in DMEM with 10% fetal bovine serum (FBS, Excell) and 1% penicillin−streptomycin (Gibco) in a humidified incubator with 5% CO_2 at 37 °C as described previously.[43]

Cell Viability Assay. The cytotoxicities were evaluated by the MTT assay as described previously.[32] Human melanoma cells SK-MEL-1 (10^4/well) were seeded in 96-well plates for 24 h and then exposed to different concentrations of compounds for 48 h, respectively. Then, after adding 10 μL of MTT solution (5 mg/mL) and incubating for another 4 h at 37 °C, the supernatant was discarded, the purple formazan crystals were dissolved in 100 μL of DMSO, and the absorbance was measured at 570 nm by a microplate reader (Multiskan FC, Thermo Scientific).

Western Blot Analysis. The protein lysates were prepared and Western blot analysis was performed as described previously.[44] SK-MEL-1 cells (3 × 10^5/well) were seeded in six-well plates for 24 h. After being treated with different concentrations of compounds **5**, **6**, and **8** for 48 h, cells were collected and washed with cold PBS and then lysed for 15 min at 4 °C with RIPA buffer (0.1 mM phenylmethanesulfonyl fluoride, 0.1 mM sodium orthovanadate, 0.1 mM dithiothreitol and phosphatase inhibitor). After centrifugation at 12 000 rpm for 15 min, supernatants were collected as total protein. The BCA assay was performed to quantify the protein concentration. Total cellular protein (20 μg) was separated by SDS-PAGE gels and then transferred to polyvinylidene fluoride membranes. After incubating with primary antibody overnight at 4 °C and secondary antibody for 1 h at room temperature, immunoreactive proteins were visualized by an ECL detection kit.

Zebrafish Embryo and Larvae Maintenance. Zebrafish were kindly provided by Professor Wenqing Zhang (Medical School at South China University of Technology, Guangzhou, China). The collection of zebrafish embryo and larvae maintenance were performed as described previously.[45] The zebrafish embryos were generated by natural pairwise mating in a light−dark cycle of 14−10 h/day (light at 8:30 am to 10:30 pm), and the zebrafish embryos and larvae were incubated at 28.5 °C in E3 medium (5 mM NaCl, 0.17 mM KCl, 0.33 mM $CaCl_2$, 0.33 mM $MgSO_4$, and 0.1% methylene blue, pH 7.0).

***In Vivo* Antiangiogenic Experiment.** Healthy zebrafish embryos (*Tg*:*Fli1-GFP* and *Tg*: *Flk1-GFP*) at 12 h postfertilization (hpf) were selected in 12-well plates with 30 embryos per well and cultured in a light incubator at 28.5 °C. At 24 hpf, the embryos were placed under the stereomicroscope (Olympus SZX7) to break the embryo membranous eggshell. Thirty six hours after the embryos were exposed to compounds, we observed the development of embryonic ISVs in zebrafish under a fluorescence microscope (Olympus MVX10) equipped with a digital camera (Olympus DP80).[33]

***In Vivo* Antitumor Experiment.** The antitumor effects of isolated compounds in SK-MEL-1 cells were confirmed by a

https://doi.org/10.1021/acs.jnatprod.0c00840
J. Nat. Prod. XXXX, XXX, XXX−XXX

xenotransplanted zebrafish model, which was established by microinjection of SK-MEL-1 cells labeled with chloromethylbenzamido-DiI (CM-DiI) into the yolk sac of 2 dpf zebrafish as described previously.[30] SK-MEL-1 cells labeled with CM-DiI were injected at the superficial location of the yolk near the perivitelline space of the embryos using a FemtoJet microinjector (PM1000 cell microinjector, MicroData Instrument, Inc.). After the treatment of compounds **5**, **6**, and **8** or sorafenib for 48 h at 28.5 °C, zebrafish were immobilized and observed by fluorescence microscopy (Olympus MVX10).

Toxicity Experiment in Zebrafish. The toxicity experiment was conducted as described previously.[46] Healthy zebrafish larvae at 48 hpf were selected and treated with compounds **1**, **2**, and **4**−**9**. The survival and pathological changes of the zebrafish larvae were observed under the stereomicroscope (Olympus SZX7) at intervals of 12 h.

Statistical Analysis. Results are from at least three independent experiments. The data were analyzed by Graph Pad Prism 6.0. Significance is considered statistical when $P < 0.05$.

■ ASSOCIATED CONTENT

Supporting Information

The Supporting Information is available free of charge at https://pubs.acs.org/doi/10.1021/acs.jnatprod.0c00840.

UV, IR, HRESIMS, and NMR spectra as well as additional crystallographic data of **2** (PDF)

Crystallographic data of **2** (CIF)

■ AUTHOR INFORMATION

Corresponding Authors

Hai-yan Tian − *Institute of Traditional Chinese Medicine and Natural Products, College of Pharmacy, Jinan University, Guangzhou 510632, People's Republic of China; Department of Chemistry and Biochemistry, University of South Carolina, Columbia, South Carolina 29208, United States;* orcid.org/0000-0002-2421-8712; Phone: 86-13760662185; Email: tianhaiyan1982@163.com

Jun-shan Liu − *Guangdong Provincial Key Laboratory of Chinese Medicine Pharmaceutics, School of Traditional Chinese Medicine, Southern Medical University, Guangzhou 510515, People's Republic of China;* orcid.org/0000-0003-3744-6180; Phone: 86-20-61648539; Email: liujunshan@smu.edu.cn

Jie Li − *Department of Chemistry and Biochemistry, University of South Carolina, Columbia, South Carolina 29208, United States;* orcid.org/0000-0001-7977-6749; Phone: 1-803-7775010; Email: LI439@mailbox.sc.edu

Authors

Shi-wen Zhou − *Institute of Traditional Chinese Medicine and Natural Products, College of Pharmacy, Jinan University, Guangzhou 510632, People's Republic of China; Department of Biomedical Sciences, City University of Hong Kong, Hong Kong, SAR 999077, People's Republic of China*

Jing-yu Quan − *Guangdong Provincial Key Laboratory of Chinese Medicine Pharmaceutics, School of Traditional Chinese Medicine, Southern Medical University, Guangzhou 510515, People's Republic of China*

Zi-wei Li − *Institute of Traditional Chinese Medicine and Natural Products, College of Pharmacy, Jinan University, Guangzhou 510632, People's Republic of China*

Ge Ye − *Institute of Traditional Chinese Medicine and Natural Products, College of Pharmacy, Jinan University, Guangzhou 510632, People's Republic of China*

Zhuo Shang − *Department of Chemistry and Biochemistry, University of South Carolina, Columbia, South Carolina 29208, United States;* orcid.org/0000-0002-5755-2629

Ze-ping Chen − *Institute of Traditional Chinese Medicine and Natural Products, College of Pharmacy, Jinan University, Guangzhou 510632, People's Republic of China*

Lei Wang − *Institute of Traditional Chinese Medicine and Natural Products, College of Pharmacy, Jinan University, Guangzhou 510632, People's Republic of China;* orcid.org/0000-0001-9242-1109

Xin-yuan Li − *Institute of Traditional Chinese Medicine and Natural Products, College of Pharmacy, Jinan University, Guangzhou 510632, People's Republic of China*

Xiao-qi Zhang − *Institute of Traditional Chinese Medicine and Natural Products, College of Pharmacy, Jinan University, Guangzhou 510632, People's Republic of China;* orcid.org/0000-0002-4436-0273

Complete contact information is available at: https://pubs.acs.org/10.1021/acs.jnatprod.0c00840

Author Contributions

#S.-W.Z. and J.-Y.Q. contributed equally to this work.

Notes

The authors declare no competing financial interest.

■ ACKNOWLEDGMENTS

This research work was financially supported by the National Natural Science Foundation of Guangdong Province, China (No. 2019A1515011489), the Guangzhou Science and Technology Plan (202002030219), the Zooming Plan of Jinan University (21615431), the Pearl River Science and Technology Program (201506010020 for H.-Y.T. and 201710010026 for J.-S.L.), the Guangdong Province Universities and Colleges Pearl River Scholar Funded Scheme (GDHVPS2018), the Guangdong National Natural Science Funds for Distinguished Young Scholar (2017A030306006), the National Natural Science Foundation of China (U1801287), National Institutes of Health (NIH) grant P20GM103641, and the National Science Foundation EPSCoR Program OIA-1655740.

■ REFERENCES

(1) Schmidt, B. R.; Hodl, W.; Schaub, M. *Ecology* **2012**, *93*, 657−667.
(2) Ujvari, B.; Casewell, N. R.; Sunagar, K.; Arbuckle, K.; Wuster, W.; Lo, N.; O'Meally, D.; Beckmann, C.; King, G. F.; Deplazes, E.; Madsen, T. *Proc. Natl. Acad. Sci. U. S. A.* **2015**, *112*, 11911−11916.
(3) Steyn, P. S.; van Heerden, F. R. *Nat. Prod. Rep.* **1998**, *15*, 397−413.
(4) Gao, H. M.; Popescu, R.; Kopp, B.; Wang, Z. M. *Nat. Prod. Rep.* **2011**, *28*, 953−969.
(5) Prassas, I.; Diamandis, E. P. *Nat. Rev. Drug Discovery* **2008**, *7*, 926−935.
(6) Editorial Committee of the Administration Bureau of Traditional Chinese Medicine. In *Chinese Materia Medica (ZhonghuaBencao)*; Shanghai Science and Technology Press: Shanghai, 1999; pp 362−367.
(7) Zhakeer, Z.; Hadeer, M.; Tuerxun, Z.; Tuerxun, K. *Pharmacology* **2017**, *99*, 179−187.
(8) Qi, J.; Tan, C. K.; Hashimi, S. M.; Zulfiker, A. H.; Good, D.; Wei, M. Q. *Evid. Based Complement. Alternat. Med.* **2014**, *2014*, 312684.

(9) Zhu, Z. T.; Li, E.; Liu, Y. Y.; Gao, Y.; Sun, H. Z.; Wang, Y.; Wang, Z. H.; Liu, X. M.; Wang, Q. J.; Liu, Y. P. *Acta Haematol.* **2012**, *128*, 144−150.
(10) Zhang, D. M.; Liu, J. S.; Deng, L. J.; Chen, M. F.; Yiu, A.; Cao, H. H.; Tian, H. Y.; Fung, K. P.; Kurihara, H.; Pan, J. X.; Ye, W. C. *Carcinogenesis* **2013**, *34*, 1331−1342.
(11) Zhou, S. W.; Zheng, Q. F.; Huang, X. Y.; Wang, Y.; Luo, S. F.; Jiang, R. W.; Wang, L.; Ye, W. C.; Tian, H. Y. *Org. Biomol. Chem.* **2017**, *15*, 5609−5615.
(12) Zhan, X.; Wu, H.; Wu, H.; Wang, R.; Luo, C.; Gao, B.; Chen, Z.; Li, Q. *J. Ethnopharmacol.* **2020**, *246*, 112178.
(13) Liu, J.; Zhang, D.; Li, Y.; Chen, W.; Ruan, Z.; Deng, L.; Wang, L.; Tian, H.; Yiu, A.; Fan, C.; Luo, H.; Liu, S.; Wang, Y.; Xiao, G.; Chen, L.; Ye, W. *J. Med. Chem.* **2013**, *56*, 5734−5743.
(14) Hayes, R. A.; Crossland, M. R.; Hagman, M.; Capon, R. J.; Shine, R. *J. Chem. Ecol.* **2009**, *35*, 391−399.
(15) Zhang, P. W.; Tian, H. Y.; Nie, Q. L.; Wang, L.; Zhou, S. W.; Ye, W. C.; Zhang, D. M.; Jiang, R. W. *RSC Adv.* **2016**, *6* (96), 93832−93841.
(16) Yang, Y.; Gu, C.; Ding, N.; Wang, Y.; Ren, H. CN Patents CN2017-10160554, CN106946967, and CN20170317, 2017.
(17) Zhao, J.; Guan, S. H.; Chen, X. B.; Wang, W.; Ye, M.; Guo, D. A. *Chin. Chem. Lett.* **2007**, *18*, 1316−1318.
(18) Tian, H. Y.; Wang, L.; Zhang, X. Q.; Wang, Y.; Zhang, D. M.; Jiang, R. W.; Liu, Z.; Liu, J. S.; Li, Y. L.; Ye, W. C. *Chem. Eur. J.* **2010**, *16*, 10989−10993.
(19) Li, B. J.; Tian, H. Y.; Zhang, D. M.; Lei, Y. H.; Wang, L.; Jiang, R. W.; Ye, W. C. *Fitoterapia* **2015**, *105*, 7−15.
(20) Tian, H. Y.; Ruan, L. J.; Yu, T.; Zheng, Q. F.; Chen, N. H.; Wu, R. B.; Zhang, X. Q.; Wang, L.; Jiang, R. W.; Ye, W. C. *J. Nat. Prod.* **2017**, *80*, 1182−1186.
(21) Chen, H.; Meng, Y. H.; Guo, D. A.; Liu, X.; Liu, J. H.; Hu, L. H. *Fitoterapia* **2015**, *104*, 1−6.
(22) Ye, M.; Qu, G. Q.; Guo, H. Z.; Guo, D. *J. Steroid Biochem. Mol. Biol.* **2004**, *91*, 87−98.
(23) Kamano, Y.; Kotake, A.; Takano, R.; Morita, H.; Takeya, K.; Itokawa, H. *Heterocycles* **1998**, *49*, 275−280.
(24) Hutchinson, D. A.; Mori, A.; Savitzky, A. H.; Burghardt, G. M.; Wu, X.; Meinwald, J.; Schroeder, F. C. *Proc. Natl. Acad. Sci. U. S. A.* **2007**, *104*, 2265−2270.
(25) Tempone, A. G.; Pimenta, D. C.; Lebrun, I.; Sartorelli, P.; Taniwaki, N. N.; de Andrade, H. F., Jr.; Antoniazzi, M. M.; Jared, C. *Toxicon* **2008**, *52*, 13−21.
(26) Li, H. N.; Cao, X. R.; Lin, X. J.; Chen, X. B.; Yi, X. H.; Xia, J.; Chen, J. L.; Yang, L. *Mol. Med. Rep.* **2019**, *20*, 2347−2354.
(27) Hseu, Y. C.; Cho, H. J.; Gowrisankar, Y. V.; Thiyagarajan, V.; Chen, X. Z.; Lin, K. Y.; Huang, H. C.; Yang, H. L. *Free Radical Biol. Med.* **2019**, *143*, 397−411.
(28) Mattia, G.; Puglisi, R.; Ascione, B.; Malorni, W.; Care, A.; Matarrese, P. *Cell Death Dis.* **2018**, *9*, 112.
(29) Kamano, Y.; Yamashita, A.; Nogawa, T.; Morita, H.; Takeya, K.; Itokawa, H.; Segawa, T.; Yukita, A.; Saito, K.; Katsuyama, M.; Pettit, G. R. *J. Med. Chem.* **2002**, *45*, 5440−5447.
(30) Smulson, M. E.; Simbulan-Rosenthal, C. M.; Boulares, A. H.; Yakovlev, A.; Stoica, B.; Iyer, S.; Luo, R.; Haddad, B.; Wang, Z. Q.; Pang, T.; Jung, M.; Dritschilo, A.; Rosenthal, D. S. *Adv. Enzyme Regul.* **2000**, *40*, 183−215.
(31) Li, M. M.; Wu, S.; Liu, Z.; Zhang, W.; Xu, J.; Wang, Y.; Liu, J. S.; Zhang, D. M.; Tian, H. Y.; Li, Y. L.; Ye, W. C. *Biochem. Pharmacol.* **2012**, *83*, 1251−1260.
(32) Liu, J. S.; Huo, C. Y.; Cao, H. H.; Fan, C. L.; Hu, J. Y.; Deng, L. J.; Lu, Z. B.; Yang, H. Y.; Yu, L. Z.; Mo, Z. X.; Yu, Z. L. *Phytomedicine* **2019**, *61*, 152843.
(33) Wang, C.; Tao, W.; Wang, Y.; Bikow, J.; Lu, B.; Keating, A.; Verma, S.; Parker, T. G.; Han, R.; Wen, X. Y. *Eur. Urol.* **2010**, *58*, 418−426.
(34) Camus, S.; Quevedo, C.; Menendez, S.; Paramonov, I.; Stouten, P. F.; Janssen, R. A.; Rueb, S.; He, S.; Snaar-Jagalska, B. E.; Laricchia-Robbio, L.; Izpisua Belmonte, J. C. *Oncogene* **2012**, *31*, 4333−4342.
(35) Wiens, K. M.; Lee, H. L.; Shimada, H.; Metcalf, A. E.; Chao, M. Y.; Lien, C. L. *PLoS One* **2010**, *5*, e11324.
(36) Habeck, H.; Odenthal, J.; Walderich, B.; Maischein, H.; Schulte-Merker, S.; Tubingen screen, c. *Curr. Biol.* **2002**, *12*, 1405−1412.
(37) Zhang, B.; Shimada, Y.; Hirota, T.; Ariyoshi, M.; Kuroyanagi, J.; Nishimura, Y.; Tanaka, T. *Transl. Res.* **2016**, *170*, 89−98.
(38) Haldi, M.; Ton, C.; Seng, W. L.; McGrath, P. *Angiogenesis* **2006**, *9*, 139−151.
(39) Tian, H. Y.; Wang, L.; Zhang, X. Q.; Zhang, D. M.; Wang, Y.; Liu, J. S.; Jiang, R. W.; Ye, W. C. *Steroids* **2010**, *75*, 884−890.
(40) Dolomanov, O. V.; Bourhis, L. J.; Gildea, R. J.; Howard, J. A. K.; Puschmann, H. *J. Appl. Crystallogr.* **2009**, *42*, 339−341.
(41) Sheldrick, G. M. *Acta Crystallogr., Sect. A: Found. Crystallogr.* **2008**, *64*, 112−122.
(42) Sheldrick, G. M. *Acta Crystallogr., Sect. C: Struct. Chem.* **2015**, *71*, 3−8.
(43) Liu, J. S.; Wei, X. D.; Wu, Y. F.; Wang, Y. N.; Qiu, Y. W.; Shi, J. M.; Zhou, H. L.; Lu, Z. B.; Shao, M.; Yu, L. Z.; Tong, L. *Cell. Oncol.* **2016**, *39*, 333−342.
(44) Lu, Z. B.; Xie, P.; Zhang, D. M.; Sun, P. H.; Yang, H. Y.; Ye, J. X.; Cao, H. H.; Huo, C. Y.; Zhou, H. L.; Chen, Y. Y.; Ye, W. C.; Yu, L. Z.; Liu, J. S. *Biochem. Pharmacol.* **2018**, *158*, 305−317.
(45) Gan, L.; Zheng, Y.; Deng, L.; Sun, P.; Ye, J.; Wei, X.; Liu, F.; Yu, L.; Ye, W.; Fan, C.; Liu, J.; Zhang, W. *Molecules* **2019**, *24*, 2726.
(46) Jagadeeshan, S.; Sagayaraj, R. V.; Paneerselvan, N.; Ghouse, S. S.; Malathi, R. *Cell Biol. Toxicol.* **2017**, *33*, 41−56.

https://doi.org/10.1021/acs.jnatprod.0c00840
J. Nat. Prod. XXXX, XXX, XXX−XXX